A STUDY OF METEOR ECHOES AT HF USING THE BEAR LAKE DYNASONDE

C.S. Fish and F.T. Berkey
Space Dynamics Laboratory
Utah State University
Logan, UT 84322-4145

ABSTRACT

The occurrence of short-lived sporadic E (E_s) events at rates up to several per hour have been observed in ionograms recorded by the NOAA dynasonde operated at Utah State University's (USU) Bear Lake Observatory (41.9°N, 111.4°W). Because these E_s events tend to occur predominantly between local midnight and early afternoon, have a wide radio bandwidth, and occur at ranges <150 km, a meteoric origin is assumed. While many E_s events are very short-lived and detected only over a narrow frequency range, numerous events exhibiting wide radio bandwidths have been observed. Conventional meteor radar systems typically operate in the VHF range, although several studies have been conducted using HF radars, where the duration of the echoes is much longer. While direct reflections from individual meteor ionization trains are not uncommon in vertical incidence HF sounding, relatively few reports have appeared in the literature. In this paper, we utilize the full vector capabilities of the dynasonde to derive meteor echo amplitude, height distribution, temporal duration, and Doppler shift as a function of frequency from data collected during the Leonids shower of November 17 and 18, 1998.

Introduction

Short-lived E_s events are frequently observed in ionograms recorded by the USU dynasonde with occurrence rates of up to several per hour. These E_s events are most evident between the hours of local midnight and early afternoon and are characterized by radio bandwidths up to several MHz (4-5 MHz). They generally occur at heights below 150 km with a peak at approximately 105 km, strongly suggesting a meteoric origin. The variation of E_s activity with meteoric flux has been studied using ionosonde data from three sites [*Wright*, 1967] and sporadic-E ionization associated with meteor events has been more recently investigated by *Rajaram and Chandra* [1991]. Radar observations of the trails of ionization created by meteors incident upon the Earth's upper atmosphere provide a means of investigating the physics of meteors [*Verniani*, 1973] as well as serving as useful tools for probing the dynamics of the D and E regions of the ionosphere. While most of the published work has been derived from VHF meteor radars, there have been a number of notable exceptions [*Steel and Elford*, 1991]. In this paper, we present observations of meteor echoes made with the USU dynasonde operating in fixed-frequency mode.

Meteor Physics

As a meteor enters the Earth's atmosphere, it collides with air molecules that become trapped on its surface. Heat from the collisions ablates (evaporates) atoms from the meteor which in turn collide with surrounding air molecules. These sum of these collisions produces heat, light, and a trail of ionization. Ablated (vaporized) meteor atoms travel at meteoric velocities for a short time and almost instantaneously form a ionized trail with an initial radius r_o. Complete meteor evaporation generally occurs between 70 and 150 km (e.g. the meteor region). In some cases, meteors break into smaller particles (fragment) and then proceed as a group, in which case each particle is treated as an individual meteor. An empirical relationship between the initial trail radius r_o and meteor height can be written as

$$r_o = 10^{(.035h-3.25)} \quad (1)$$

where h is in km [*CCIR*, 1986]. After a trail forms, it expands at a relatively low rate by ambipolar diffusion, creating a radial distribution of ionization that is approximately Gaussian. The ambipolar diffusion constant, D, increases with height in the meteor region. *Greenhow and Neufeld* [1955], developed an empirical relation between the ambipolar diffusion constant and height given as

$$D = 10^{(.067h-5.6)} \quad (2)$$

where h is in km. After a time t, the approximate radius of the trail r due to ambipolar diffusion is related to r_o by

$$r^2 = r_0^2 + 4Dt \qquad (3)$$

Sugar [1964].

Ionized meteor trails are divided into two general classes - underdense and overdense - based on their radio wave reflection properties. In the case of underdense trails, the electron line density, q, is low enough such that an incident radio wave passes through the trail and the trail is only considered as a partial reflector. For overdense trails, q is high enough to prevent complete penetration of the incident radio wave. The wave is then reflected in the same manner as seen in ionospheric layer radio wave reflections.

The returned echo power from an underdense trail received by a monostatic radar is

$$P_R(t) = [\frac{P_T(t)G^2\lambda^3 q^2 r_e^2}{32R_0^3}]\exp(\frac{-8\pi^2 R_0^2}{\lambda^2})\exp(\frac{-32\pi^2 Dt}{\lambda^2}) \quad (4)$$

where R_o is the minimum distance between the radar and the meteor trail when the radar beam is normal to the trail and r_e is the classical electron radius [*Sugar*, 1964]. The received power is immediately reduced by the factor expressed contained in the first exponential due to the initial trail radius, and decays thereafter according to the time-varying diffusion factor (the function of the second exponential), also called the e-folding constant [*Zhou et al.*, 1998]. $P_R(t)$ is proportional to the square of the line density. As the trail expands through ambipolar diffusion, the phase difference from reflections on both sides of the trail increases, resulting in a decrease in signal strength. The time taken for $P_R(t)$ to decay by a factor of e^{-2} is called the amplitude decay time, T_{un}, and is given by

$$T_{un} = \frac{\lambda^2}{16\pi^2 D} \qquad (5)$$

[*McKinley*, 1961]. The theoretical decay time is independent of all parameters at a given height except radio wavelength, so that T_{un} will be the same for all meteors as long as the line densities in the trail remain underdense. Underdense echo duration is typically on the order of fractions of a second.

From radar observations of underdense meteor echoes at 54.1, 26.4, 6, and 2 MHz, *Steel and Elford* [1991] suggest that the peak meteor ionization height may lie somewhere near 125 km. They also determined average echo detection heights as a function of frequency, finding means at 93 and 95 km for 54.1 and 24.6 MHz, respectively and ≈105 for both 2 and 6 MHz. However the upper limit of detection for the lower frequencies was limited due to atmospheric and experimental considerations.

The critical electron density, N_c, defining the transition from underdense to overdense ionization, occurs when the dielectric constant of the cylinder-like trail is equal to zero. The transition line density, q_{tr}, denotes the crossing electron line density from underdense to overdense trails and is on the order of 10^{14} electrons per meter [*McKinley*, 1961]. For a line density q greater than or equal to q_{tr}, the meteor trail is considered overdense and will generally produce an overdense echo. However, if the incident wave frequency is high enough (e.g. the upper end of the VHF band) or the height of the meteor large (≥120 km), the echo power received from an overdense trail may exhibit the characteristics of an underdense trail [*McKinley*, 1961; *Sugar*, 1964]. Overdense echo observations are possible only after the trail has reached its initial radius. Under either of the above conditions, the volume density along the trail axis at that instant when r_o is attained may be below the requirements for an overdense echo. Therefore, the defining condition for an overdense echo to be obtained from an overdense trail is that the overdense echo duration, T_{ov}, must be greater than the time which would be taken for the meteor trail to expand to r_o were ordinary diffusion the only process involved [*Manning*, 1958]. The overdense echo time duration, for which the echo amplitude is relatively constant, is given by

$$T_{ov} \approx \frac{\lambda^2 q}{4\pi^3 D q_{tr}} \qquad (6)$$

[*McKinley*, 1961]. The power received by a monostatic radar from an overdense meteor trail is

$$P_R(t) = [\frac{P_T(t)G^2\lambda^2}{64\pi^2 R_0^2}]\sqrt{4Dt * \ln(\frac{r_e q \lambda^2}{4\pi^2 Dt})} \qquad (7)$$

[*Sugar*, 1964], where the power is proportional to the square root of T_{ov}. Overdense echoes can persist for intervals up to several minutes, with most maintaining a relatively constant amplitude for several seconds.

Fading effects associated with "glints" and "blobs" are often observed in long-enduring echoes from overdense meteor trails. Long-wavelength, long-enduring trails can be distorted by wind shears in the upper atmosphere. Large-scale (order of 1 km) wind shears can rotate the

trail by 90º in tens of seconds [*Eshleman*, 1960], creating distortion which causes localized points (glints) along the meteor trail where Fresnel-zone reflections may occur. The waves scattered from various glints interfere at the receiver and cause fading of the meteor echo. *Booker and Cohen* [1956] have suggested that local trail expansion and scattering properties are influenced by small-scale (on order of 1m), which renders each portion of the trail rough (blobs) in approximately half a second. This turbulence may be due to meteor fragmentation. These rough regions cause reflection regardless of trail orientation. *McKinley and Millman* [1949] indicate that glints are more likely to be the dominant mechanism of fading and that the inclusion of blobs helps to explain the observed pattern of fading in radar measurements from overdense trails.

While the columns of ionization left by meteors generally produce specular reflections, nonspecular echoes sometimes appear that exhibit no appreciable enduring characteristics and move with the velocity of the meteor. *McKinley and Millman* [1949b] called thistype of meteor echo a "head echo." The amplitude variation associated with head echoes is usually much smaller than that predicted by diffraction theory [*McKinley*, 1955], which is applicable to echoes from columns of ionization. Observed head echoes generally are approaching the radar, however receding head echoes are sometimes detected. Often, both head and body (trail) echoes are seen together, with the body echo appearing within 0.5-30 seconds after the head echo [*McIntosh*, 1962; *McKinley*, 1961, *Zhou et al.*, 1998]. After four decades of research, there is still no comprehensive theory which explains all the features associated with the head echo [*Jones and Webster*, 1991].

Meteor Echo Observations

Figures 1-4 show examples of typical meteor echo observations obtained from fixed-frequency P-mode soundings recorded by the Bear Lake dynasonde. The soundings were repeated at 5 minute intervals and made on two separate frequencies; 3.8 MHz (1600-2400UT) and 2.2 MHz (0000-1559UT). The IPP was 0.08 seconds and the height resolution for each echo is ±0.75 km. Each sounding lasted approximately 80 seconds. The data shown here were acquired during the Leonids meteor shower on November 17 and 18, 1998. Figures 1(a-g) and 3(a-e) depict the signal amplitude and phase values for underdense and overdense echoes, respectively. Figures 2(a,b) show the measured ambipolar diffusion and e-folding constants for the underdense echoes recorded over the two day period. Figures 4(a,b) illustrate signal amplitude as a function of time, and contain examples of both underdense and overdense echoes.

Underdense Echoes

In Figures 1(a-f), the signal phase has been unwrapped, so that the total phase change (in radians) is shown. The time scale is in seconds relative to the start of the sounding. The decay of the echo amplitude follows closely the predicted behavior given by equation (4). Even though the echoes were recorded at fairly high altitudes where the ambipolar diffusion constant is large, the decay times are on the order of seconds due to the long radio wavelengths. The measured echo-amplitude decay time, T_{unm}, was determined for each echo based on an amplitude decrease of 8.7 dB from the initial peak amplitude. Comparisons between T_{unm} and the predicted T_{un} as given by equation (5) are listed in Table 1. The ambipolar diffusion constant used in equation (5) was calculated from equation (2). Both measured and predicted decay times are nearly equal in all the cases.

The change in phase of the signal with respect to time during the decay period denotes the induced neutral wind speed of the approaching or receding trail, V_{radial}. From Doppler theory, this is expressed as

$$V_{radial} = -\left(\frac{\lambda}{2\pi}\right)\left(\frac{\delta\phi}{\delta t}\right) \qquad (8)$$

where ø is the phase of the returned echo signal [*Cervera and Reid*, 1995]. The values of the measured radial velocities, $V_{radialm}$, for each echo are also listed in Table 1.

Figures 2(a,b) show scatter plots of the ambipolar diffusion and e-folding constants of the underdense echoes detected during the November 17-18 soundings. The triangles denote the measured values and the solid line shows the predicted value; the measurements fit the predicted curve rather nicely. It is apparent that many more echoes were detected at 3.8 MHz than at 2.2 MHz. Since the soundings began at 18:46 UT on November 17 and finished at 19:01 UT on November 18, the number of hours for which soundings were made at each frequency was approximately equal. To date, we have been

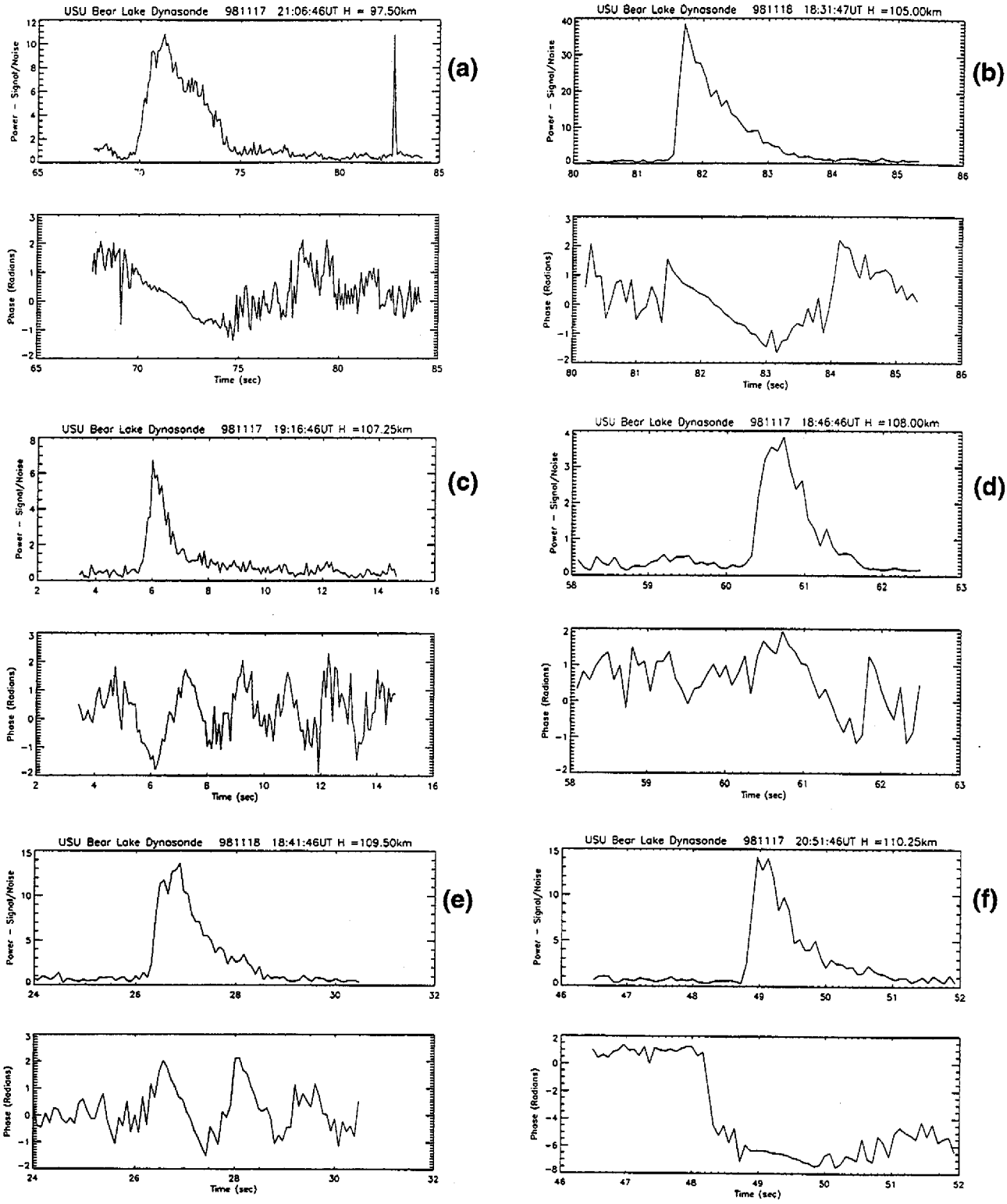

Figure 1. Amplitude and Phase Characteristics of Underdense Echoes
The amplitude and phase, as functions of time, of underdense meteor echoes detected during six separate soundings are shown in the upper and lower panels of events (a) - (f). Each event is annotated with the date, time and height at which the echo was observed.

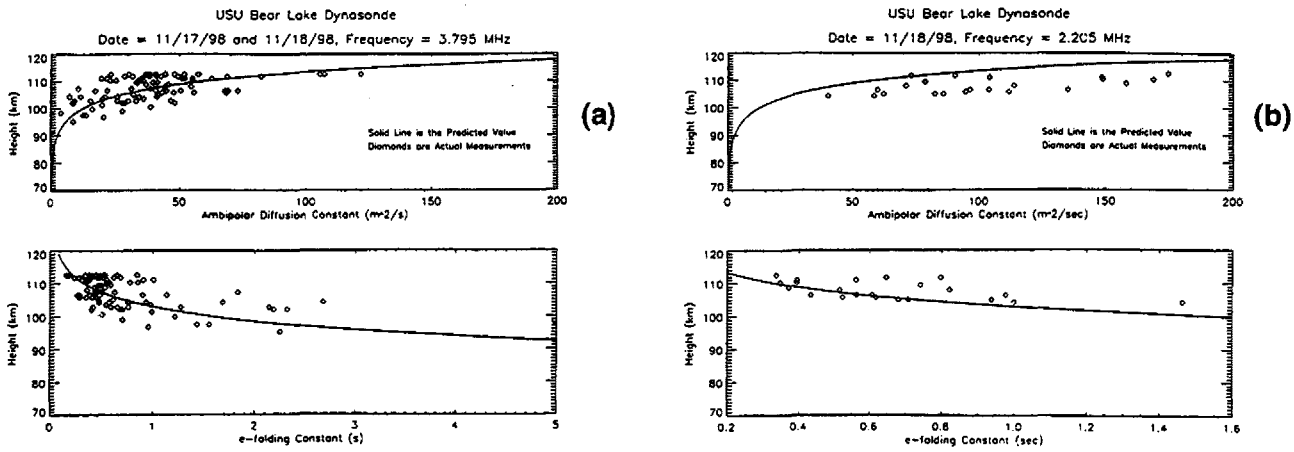

Figure 2. Ambipolar Diffusion and e-folding Constants of Underdense Meteor Echoes The ambipolar diffusion and e-folding constants, as functions of height, for underdense meteor echoes detected during soundings at 3.8 MHz and 2.2 MHz are shown in the upper and lower panels of events (a) and (b). Triangles denote the measured values and the solid lines represent predictions.

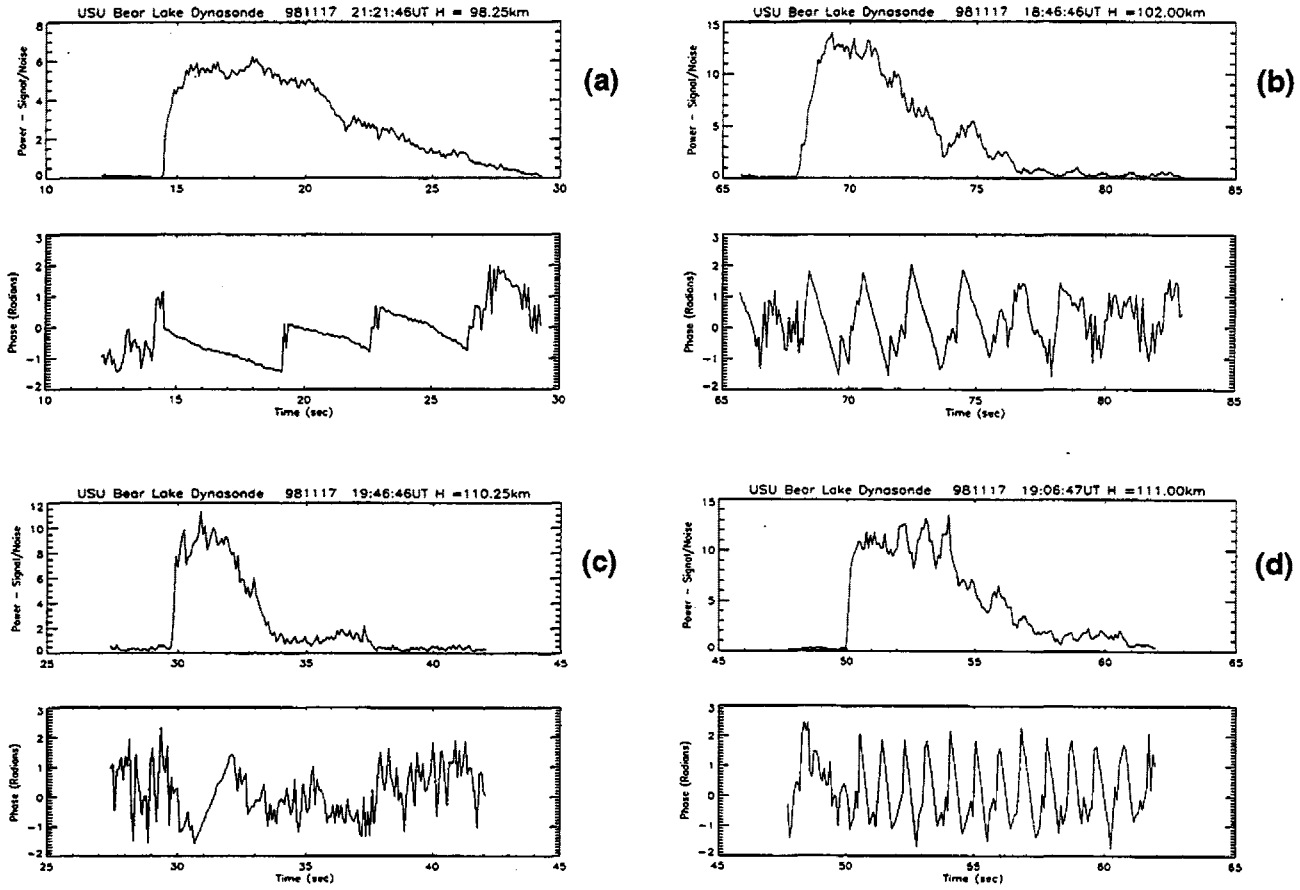

Figure 3. Amplitude and Phase Characteristics of Overdense Meteor Echoes The amplitude and phase, as functions of time, of overdense meteor echoes detected during four separate soundings are shown in the upper and lower panels of events (a) - (d). Each event is annotated with the date, time and height at which the echo was observed.

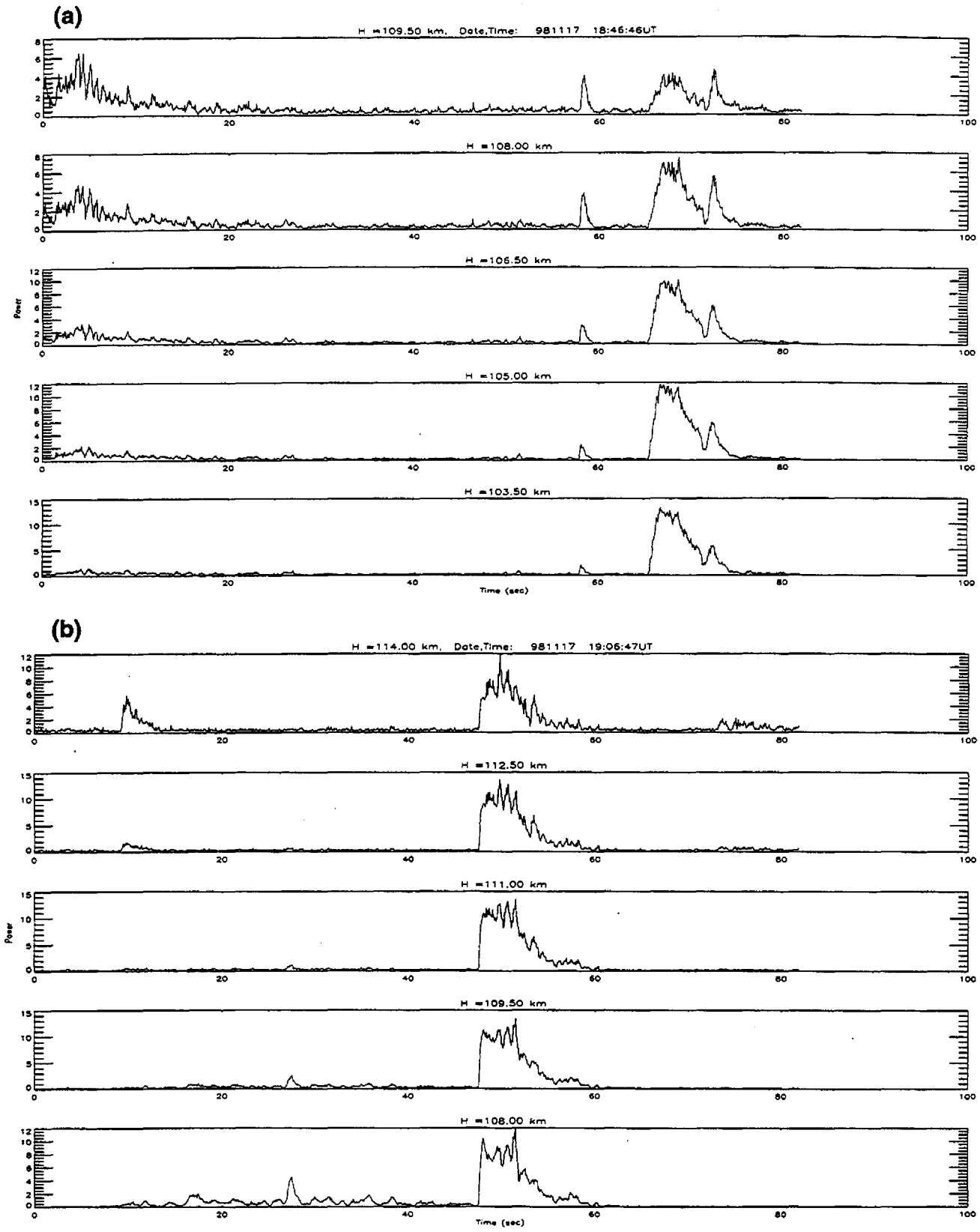

Figure 4. Time Series Range Plots

The amplitude, as a function of time, of overdense and underdense meteor echoes detected during two separate soundings, over five range gates, is shown in the panels of events (a) and (b). Each event is annotated with the height, date, and time of the sounding.

Table 1. Underdense Echo Characteristics

Altitude, km	Time, UT	Date	Figure	D, m^2s^{-1}	T_{umm}, s	T_{un}, s	$V_{radialm}$, m/s
97.50	21:06	17	1(a)	8.56	3.90	4.62	7.11
105.00	18:31	18	1(b)	27.22	1.30	1.45	25.16
107.25	19:16	17	1(c)	38.52	1.15	1.02	-43.96
108.00	18:46	17	1(d)	43.25	0.81	0.92	42.54
109.50	18:41	18	1(e)	54.51	1.00	0.73	53.28
110.25	20:51	17	1(f)	61.19	0.80	0.64	14.93

Table 2. Overdense Echo Characteristics

Altitude, km	Time, UT	Date	Figure	D, m^2s^{-1}	T_{ovm}, s	q/q_{tr}
98.25	21:21	17	3(a)	9.61	6.00	1.14
102.00	18:46	17	3(b)	17.14	2.90	0.99
110.25	19:46	17	3(c)	61.19	2.20	2.73
111.00	19:06	17	3(d)	68.71	4.00	5.45

unable to determine the cause of this discrepancy (i.e. time of day, season, local radio interference, and transmitter-receiver parameters), but the results suggest that future measurements should be made at 3.8 MHz and/or another frequency other than 2.2 MHz.

Approximately 30 underdense echoes per hour were recorded at 3.8 MHz. Nearly half of these were rejected for further analysis due to decay constants that were either too short or too long. The average height at which echoes were detected was 105 km, which is identical to the results of *Steel and Elford* [1991] for similar radio frequencies.

Overdense Echoes

The time over which the amplitude was constant for the overdense trail echoes shown in Figures 3(a-d) , T_{ovm}, was used to calculate q/q_{tr}; these values are listed in Table 2. For all echoes except Figure 3(b), the ratio q/q_{tr} was greater than unity. A radial trail velocity was not measured for the overdense echoes, since long-enduring overdense echoes are subject to effects from blobs and glints, as noted previously and the multiple reflection points that result can produce signals that beat with each other. Furthermore, the winds may also be strong enough to rotate the trail away from the specular reflection condition [*Cervera and Reid*, 1995]. The echoes in Figures 3(a, b, and e) are suggestive of the beating effect and all of the overdense echo amplitudes show signs of distortion to varying degrees.

The measurements of signal amplitude shown in Figures 4(a-b) contain typical signatures of both underdense and overdense echoes. For example, there appears to be four separate meteors in Figure 4(a) evolving at different times and ranges. An overdense echo, appearing at the beginning of the sounding, is followed by the appearance of an underdense echo at ≈58 seconds. Between ≈65-75 seconds, both overdense and underdense echoes occur. In Figure 4(b) multiple echoes also occur; with an overdense echo appearing at ≈10 seconds. A second underdense echo occurs at ≈27 seconds, followed by a strong overdense echo at 48 seconds.

Conclusions

In this study, it has been demonstrated that NOAA dynasonde can be used to detect meteors near 4 MHz. Using P-mode sounding acquired on November 17-18, 1998, we detected both underdense and overdense echoes. The soundings were made at 2.2 MHz in the night and early morning and at 3.8 MHz in the afternoon. A majority of the underdense echoes were detected at 3.8 MHz with an average detection height of

105 km. Approximately 30 underdense echoes per hour were detected, half of which were suitable for analysis. We used the measured amplitude and phase of the underdense echoes to derive the echo amplitude decay times, ambipolar diffusion constants, e-folding constants, and radial velocities due to neutral winds. The resulting decay times and the ambipolar and e-folding constants are consistent with the predicted values. The line density ratio for the overdense echoes was calculated from measured constant-amplitude echo durations and found to agree closely with the theoretical values.

The dynasonde also has the capability to measure the spatial location of the meteor trail echoes. If a sufficiently large number of underdense echoes can be detected, the neutral winds can be derived from the radial Doppler velocity of the meteor trails. Future objectives are to employ the spatial echo mapping abilities of the dynasonde, to determine the most suitable frequency for echo detection, and to increase the frequency and/or time duration of the P-mode soundings for increased meteor detection capability. This should give us the capability of deriving the neutral winds. We also wish to implement and utilize the "pre-t_o phase technique" for meteor velocity determination as outlined by *Cervera et al.* [1997].

Acknowledgments: This work has been sponsored by the Rocky Mountain Space Grant Consortium and the National Science Foundation, by grant OPP-953095 from the Office of Polar Programs and grant ATM-9525818 from the Division of Atmospheric Sciences. The authors are indebted to G.O.L. Jones and other staff of the British Antarctic Survey for providing assistance in implementing the IDI technique.

References

Booker, H.G., and R. Cohen, *J. Geophys. Res.*, **61**, 707-733, 1956.

Cervera, M.A. and I.M. Reid, *Radio Sci.*, **30**(4), 1245-1261, 1995.

Cervera, M.A., W.G. Elford, and D.I. Steel, *Radio Sci.*, **32**(2), 805-816, 1997.

CCIR, Propagation in Ionized Media. Recommendations and Reports of the CCIR. 1986 VI., Int. Telecom. Union, Geneva, 1986.

Eshleman, V.R., Meteor Scatter, in ***The Radio Noise Spectrum***, edited by D.H. Menzel, 49-78, Harvard University Press, Cambridge, Massachusetts, 1960.

Greenhow, J.S., and E.L. Neufeld, *J. Atmos. Terr. Phys.*, **6**, 133-140, 1955.

Jones, J., and A.R. Webster, *Planet. Space Sci.*, **39**(6), 873-878, 1991.

Manning, L.A., *J. Geophys. Res.*, **63**(1), 181-196, 1958.

McIntosh, B.A., *J. Atmos. Terr. Phys.*, **24**, 311-315, 1962.

McKinley, D.W.R., and P.M. Millman, *Proc. I.R.E.*, **37**, 364-375, 1949.

McKinley, D.W.R. and P.M. Millman, *Can. J. Phys.*, **A27**, 53-67, 1949b.

McKinley, D.W.R., *Spec. Supp. J. Atmos. Terr. Phys.*, **2**, 65-72, 1955.

McKinley, D.W.R., ***Meteor Science and Engineering***. McGraw-Hill, New York, 1961.

Rajaram, G., and H. Chandra, *Proc. Indian Acad. Sci. (Earth Planet. Sci.)*, **100**, 255-265, 1991.

Steel, D.I., and W.G. Elford, *J. Atmos. Terr. Phys.*, **53**(5), 409-417, 1991.

Sugar, G.R., *Proc. IEEE*, **52**(2), 117-136, 1964.

Verniani, F., *J. Geophys. Res.*, **78**, 8429-8462, 1973

Wright, J. W., *J. Geophys. Res.*, **72**, 4821-4829, 1967

Zhou, Q.H., P. Perillat, J.Y.N. Cho, and J.D. Mathews, *Radio Sci.*, **33**(6), 1641-1654, 1998.